

Three-Phase Time-Domain Simulation of Very Large Distribution Networks

Vitaly Spitsa, *Member, IEEE*, Reynaldo Salcedo, *Student Member, IEEE*, Xuanchang Ran, Juan F. Martinez, *Member, IEEE*, Resk Ebrahim Uosef, *Member, IEEE*, Francisco de León, *Senior Member, IEEE*, Dariusz Czarkowski, *Member, IEEE*, and Zivan Zabar, *Senior Member, IEEE*

Abstract—This paper presents a detailed three-phase analysis of very large real-life distribution networks using the Electromagnetic Transients Program (EMTP). All main network elements, including relay protection devices, are accurately modeled considering their control sequences. Model validation is achieved with steady-state and transient simulations. The time-domain results are compared with field-validated load-flow simulations for several loading conditions including first and second contingencies. Simulations of fault conditions are also matched against known results at different locations around the network. Moreover, time-domain simulations of recorded transient events show very good agreement. Different transient scenarios are investigated. The new program can be used for the assessment of symmetrical as well as unsymmetrical faults, for studies of different switching scenarios, penetration of distributed generation, and smart grid technologies.

Index Terms—Power distribution, power system modeling, switching transients, time-domain analysis.

I. INTRODUCTION

MODERN metropolitan distribution networks can be extremely large and complex. In the last few years, significant efforts have been made to respond to the challenges they face with smart technologies. The primary goals of these efforts concentrate on improvement of reliability, cost reduction, and better utilization of the installed equipment. Reconfigurable distribution networks with smart switching and control are considered as a promising solution [1]–[3]. Another important aspect of a modern distribution network is the introduction of distributed generation (DG) on the secondary grid. This changes the approach to system protection and operation [4]. It affects power flows, voltage profiles, and the dynamic behavior of the networks [5]. In light of the aforementioned facts, distribution networks cannot be treated as passive systems any longer. At the same time, most of the reported studies are based on steady-state methods [6]–[14]. To analyze the effect of the load modeling on DG planning, a traditional positive-se-

quence load flow was applied in [6]. An unbalanced three-phase load-flow solver was used in [7] to investigate the impact of a widespread photovoltaic generation on the distribution networks. Different formulations of an optimal power flow (OPF) were adopted in [8]–[10] to define maximum penetration levels of the DG under different physical constraints. Evolutionary algorithms for sizing and placement of distributed power sources were presented in [11] and [12]. Analytical rules for the same design objectives were derived in [13] and [14].

When new control and operation strategies are to be applied to the real-life large-scale networks (to eliminate the possibility of unpredicted system behavior, equipment malfunctioning, and faults), they must be verified using accurate dynamic models. A variety of simulation tools exists for power system time-domain analysis [15], [16]. They enable circuit-level modeling and precise reconstruction of electrical variable waveforms. However, in many cases, the application of these tools has been limited to relatively small networks [17]–[22]. This stems from the fact that entire networks have been modeled using only mouse-based functions of graphical user interfaces (GUIs). This approach is not suitable for a representation of extremely large systems having thousands of nodes and branches. Additional constraints were imposed by computer resources and software limitations.

Recently, an effective technique for building and maintaining time-domain models of large networks in the Electromagnetic Transients Program (EMTP) EMTP-RV [23] was reported in [24] and [25]. This technique is based on an automatic translation of text data into a GUI model using scripting (JavaScript). It was shown that the resulting model of the network can serve as a unified framework for different types of power system studies. Frequently, transient analyses are required to supplement other study techniques for the investigation of electrical networks.

In this paper, a new approach to the transient analysis of very large real-life three-phase distribution networks using the EMTP EMTP-RV is presented. Due to the size of these networks, the complexity of their interconnections, and a strict requirement of highly detailed modeling, it was impossible to perform the analysis without improving computational capabilities of the EMTP engine. Upon our request, the developers of the software had enhanced its source code and provided us with a program release having an increased maximum allowable number of subcircuits, stack and memory sizes, and improved prediction of matrix sparsity. The present time-domain studies are based on accurate modeling of all main network elements including relay protection. The process of model derivation is fully automated and involves translation of input text files extracted directly from Con Edison's databases into EMTP-RV

Manuscript received February 25, 2011; revised June 14, 2011; accepted December 01, 2011. Date of publication January 18, 2012; date of current version March 28, 2012. Paper no. TPWRD-00165-2011.

V. Spitsa, R. Salcedo, X. Ran, F. de León, D. Czarkowski and Z. Zabar are with the Electrical and Computer Engineering Department, Polytechnic Institute of New York University, Brooklyn, NY 11201 USA (e-mail: s-vitaly@hotmail.com; reynal74@aol.com; xuanchangran@hotmail.com; fdeleon@poly.edu; dcz@poly.edu; zzabar@poly.edu).

J. F. Martinez and R. E. Uosef are with Consolidated Edison Inc., New York, NY 10003 USA (e-mail: martinezj@coned.com; uosefr@coned.com).

Color versions of one or more of the figures in this paper are available online at <http://ieeexplore.ieee.org>.

Digital Object Identifier 10.1109/TPWRD.2011.2179069

netlists using a MATLAB script [26]. The proposed technique has been successfully applied to four very large distribution networks of Consolidated Edison, Inc. of New York and was found to be suitable for all 62 distribution networks of the company. Time-domain simulations for varied operating conditions, including steady state, faults, and switching scenarios are performed. The obtained results for steady state were compared to those calculated using the poly voltage load (PVL) flow program which is a proprietary software developed by Con Edison for the distribution network analysis. A complete agreement of the results confirms correctness of the created dynamic models. Currently, these models are used for validation of the next-generation (3G) smart grid concepts which are under implementation in Con Edison's distribution networks and investigation of the impact of DG penetration on operational strategies, protection, and control.

The main contribution of this paper is to present experimentally validated time-domain simulations of very large distribution networks, including substation, feeders, and secondary grid. These components are modeled and simulated with the sufficient level of precision and detail necessary to reproduce, in time domain, real-life measurements including correct sequences of operation for hundreds of relay protection devices. This paper demonstrates the fact that these days, existing software and available computational power of personal computers are enough to perform accurate transient analysis of extremely large and complex power systems which significantly facilitate implementation of the new smart grid technologies.

The rest of this paper is organized as follows. Section II describes a circuit modeling technique for very large distribution networks. The structure and operating parameters of one of the investigated Con Edison networks are presented in Section III. The results of time-domain simulation are shown and discussed in Section IV together with a comparative analysis. Finally, the conclusions of this paper are given in Section V.

II. DISTRIBUTION NETWORK MODELING

A. Typical Network Architecture

Urban distribution networks are a very complex interconnected system. For example, in New York City (NYC), such networks may contain thousands of nodes and tens of thousands of branches on both primary feeders and secondary grid. This makes the NYC distribution system unique and challenging. Its typical architecture is shown in Fig. 1. As can be seen in this figure, electrical power is supplied to the area substation that has a number of parallel transformers equipped with tap changers. A backup transformer (TR13 in Fig. 1) exists which operates when one of the main transformers is out of service. The tap changers have scheduling which depends on active power output of the transformers to the loads. The transformers are gathered into groups and can be synchronized by closing substation breakers at the synchronization (SYN) buses. There are dozens of primary feeders connecting the area substation to a secondary grid through network transformers. The feeders have breakers equipped with overcurrent relays. The network transformers operate with fixed taps. Network protectors (NPs) are installed on the secondary side of each one of the network transformers [27].

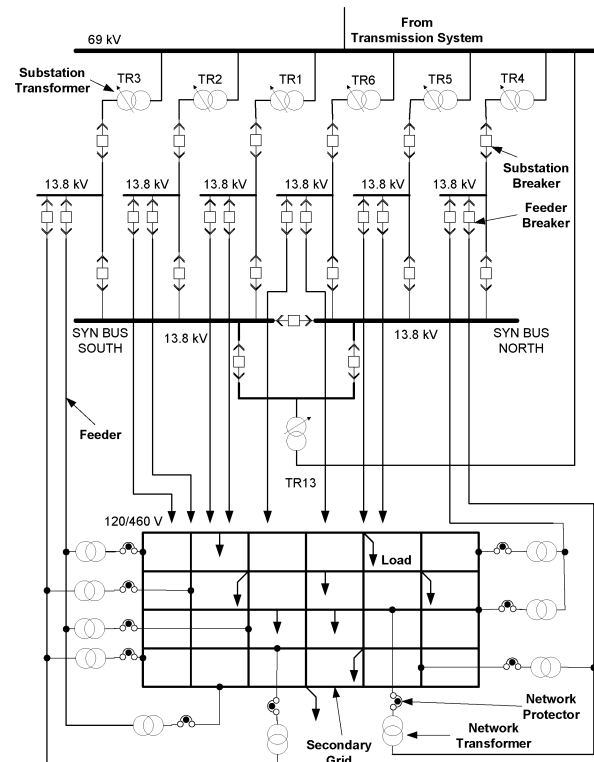


Fig. 1. Area distribution network.

These NPs prevent backfeeding from the secondary grid into the primary network. The secondary grid represents interconnections of underground cables and overhead lines supplying electrical loads. It should be noted that some of Con Edison's distribution networks have even more complex architectures since they include radial feeders, spot networks, and secondary grids at different voltage levels linked together by additional network transformers. It is obvious that manual modeling of such large and complicated networks using the graphical user interface (GUI) is impractical. In the following subsection, a new automatic modeling approach is presented. It allows generating dynamic models of distribution networks having very large size.

B. Modeling Approach

To perform time-domain simulation in any EMTP-like software, a graphical model designed using a graphical user interface (GUI) is translated first into a description language called netlist. This netlist provides information about the connectivity of the design. Since distribution networks consist of a very large number of similar elements, the following modeling approach can be adopted. The GUI of the EMTP is used only to derive detailed prototype models for each group of network elements (i.e., one model for all network transformers, one model for all breakers, and so forth). Applying this technique, the following prototype models were derived:

- area substation transformer with tap changer;
- breaker;
- overcurrent protection;
- overvoltage protection;
- undervoltage protection;
- directional power protection;

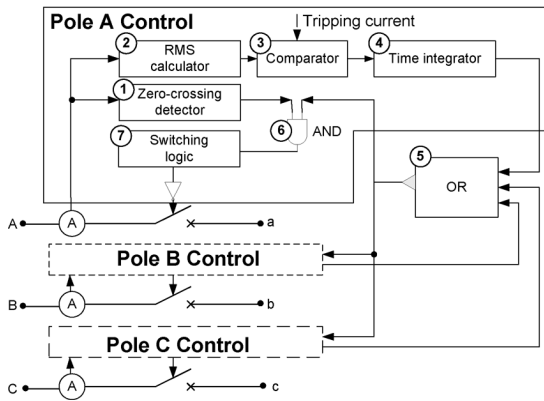


Fig. 2. Scheme of the breaker model.

- directional overcurrent protection;
- network transformer;
- network protector;
- unit substation transformers.

In addition, some built-in models in the EMTP-RV were adopted, such as PI-section, grounding zigzag transformer, RLC branch, ideal switch, and load.

The created prototype models were converted into the subcircuit netlist files. Then, the netlist generation process has been automated. The input text data files of the PVL load-flow program, which contain specifications of all network elements and connectivity information, were used to calculate the parameters, update subcircuit prototype models, and reproduce network architecture in MATLAB. For this purpose, a special script called PVL-EMTP Translator has been written. The output of this translator is a complete network netlist which can be automatically loaded into the EMTP to perform the simulation. The correctness of the derived model is verified at the result processing stage where all connections, branch impedances, network currents, and node voltages are compared to those calculated using PVL.

In the following subsections, some subcircuit prototype models are described in more detail to provide more information on model complexity.

C. Substation Transformer Model

The substation transformers are modeled according to the D/Y-reactor-grounded scheme. All of the parameters are calculated from the specification files. The model includes a precise implementation of the tap changers logic with their time delay and deadband. The secondary reference voltage is scheduled according to the measured active power of the transformer load. This load is calculated in a measurement block which outputs also the actual voltage at the secondary side of the transformer.

D. Feeder Breaker Model

Feeder breakers are represented as controlled three-phase switches. Their control logic is shown schematically in Fig. 2. As can be seen in this figure, measured rms values of the phase currents flowing through the breaker are compared with the selected tripping current. The rms values were obtained using a built-in EMTP block which calculates true rms by means of

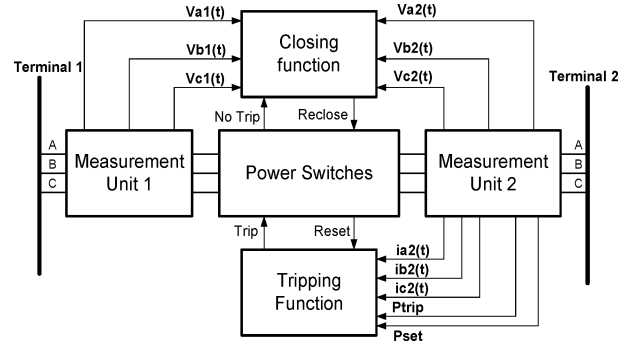


Fig. 3. Scheme of a network protector model.

numerical integration over a sliding window. Time integration is used to ensure that the tripping command will be generated only if one of the phase currents exceeds this threshold for a predefined period of time. After this period, the breaker opens when a zero crossing of the phase currents is detected after a prespecified period of time which models the mechanical delay of the device. Each breaker in the distribution network has its own tripping current and delay settings according to the specifications [28]. In addition, the developed switching logic of the model enables commanded (manual) opening and reclosing of every breaker in the network.

E. Feeder and Secondary Grid Models

Feeder conductors and secondary grid are modeled using three-phase PI sections with mutual inductances and capacitances between the phases [23]. Parameters of each section were calculated using the database information which includes section length, positive- and zero-sequence impedances, and charging reactive power.

F. Network Transformer Model

Most of the network transformers are connected D/Y-grounded and operate with fixed turn ratios. They are modeled in detail following the technique used in [29]. The network transformer models include saturation of the magnetizing curve, but not hysteresis. Parameters of each network transformer, including its nonlinear magnetizing curve, were automatically calculated from the datasheet information.

G. Network Protector Model

Network protector models in the present studies are implemented in accordance with IEEE Standard C37.06 2009 [26]. There are five functional blocks in each model. Their schematic diagram is given in Fig. 3. Two measurement blocks are used to derive information about voltages, currents, and active powers required by the tripping and closing functions. Tripping of the network protectors is primary based on reverse flow of active power from the secondary grid into the primary. The following automatic tripping functions were implemented: sensitive trip, time-delay trip, and insensitive trip.

The closing of the network protectors takes place according to the normal closing function described in [27]. Operational logic of the tripping and control functions reproduces an exact

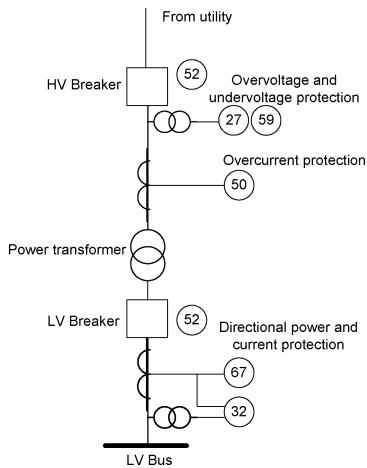


Fig. 4. High-tension customer model.

behavior of the real-life network protectors with all of the conversions and delays. Power switches are modeled with corresponding snubber circuits.

H. High-Tension Customer Model

High-tension customers are supplied by a number of power transformers connected to a common bus on the secondary side. To accurately account for the impact of these customers on the distribution network operation, they were modeled with a high level of detail according to the scheme shown in Fig. 4. The power transformer presented in this figure is modeled considering the nonlinear magnetization curve just as it was done for the network transformers. The HV breaker model is equipped with overcurrent, overvoltage and undervoltage protection relays with individual settings for each customer. Similarly, the LV breaker model on the customer side has individual relay settings of directional current and power protections.

I. Unit Substation Model

Unit substation step-down transformers are used to supply 4.16-kV subnetworks. These subnetworks do not form a secondary grid shown in Fig. 1. Instead, they represent feeders connecting different unit substations and loads distributed along them. The unit substation transformers are modeled generally just as the network transformers with the reverse current and reverse power protection installed at the secondary side.

J. Load Model

For the present studies, a built-in EMTP-RV model of electrical load has been adopted. It assumes a parallel (or series) connection of resistive and inductive elements. As a result, a constant power power-quality (PQ) load model used in PVL load-flow calculation is converted by the EMTP into a parallel RL branch placed on each phase.

K. Transmission System Model

The transmission system (including generation) is modeled using a Thevenin equivalent circuit at the high-voltage side of the area substation as it is commonly accepted for the analysis of distribution networks.

TABLE I
ELEMENTS OF THE SUTTON NETWORK

Network Element	Number
Substation transformers with tap changers	7
Shunt substation capacitors	2
Substation breakers	15
Primary feeders	12
Primary feeder sections	1,041
Primary feeder breakers	12
Network transformers	224
Network protectors	224
Secondary grid sections	1,375
Low voltage loads	311

TABLE II
LOADING CONDITIONS OF THE SUTTON NETWORK

Parameter	Units	Peak Loading	Light Loading
Active power demand	MW	143.16	48.85
Reactive power demand	Mvar	73.34	25.02
Power factor	-	0.89 (lag)	0.89 (lag)
Line charging	Mvar	1.98	1.98
Shunt capacitors	Mvar	40.0	40.0
Shunt reactors	Mvar	0.0	0.0
Total active power	MW	145.43	49.13
Total reactive power	Mvar	68.73	24.46

III. TESTED NETWORKS

A. Sutton Network

The Sutton distribution network supplies electrical loads between East 57nd and East 52nd streets from north to south, and between 1st and 5th avenues from east to west in Manhattan, NYC. An architecture of the network is shown in Fig. 1. A complete summary of all modeled elements is given in Table I. As can be concluded from this table, the Sutton network has more than two-and-a-half thousand three-phase branches (transformers as well as primary feeder and secondary grid sections). The total number of its three-phase nodes is 2333 (6999 total nodes). The transmission-side voltage of the area substation is 69 kV. The primary operates at 13.8 kV whereas electrical loads at the secondary grid consume power at voltage levels of 120/208 V.

Operational conditions of the Sutton network for peak and light loading cases are summarized in Table II. The active and reactive power demands given in this table describe an aggregate load of the distribution network. At the same time, total active and reactive powers stand for power consumption from the transmission system.

B. Flushing Network

The Flushing distribution network is located in Northern Queens, NYC. This network is probably one of the largest metropolitan distribution networks in the world. Indeed, it has 24 358 three-phase nodes, almost 30 000 three-phase branches counting feeder and secondary grid sections, and transformers. A detailed list of the elements composing the Flushing network is given in Table III. Five substation transformers are supplied

TABLE III
ELEMENTS OF THE FLUSHING NETWORK

Network Element	Number
Substation transformers with tap changers	5
Shunt substation capacitors	3
Shunt network capacitors	45
Shunt network reactors	20
Substation breakers	14
Substation capacitor breakers	3
Primary feeders	30
Primary feeder sections (with mutual couplings)	6,796
Primary feeder breakers	30
Feeder switches	30
Subnetwork switches	30
Tie switches	13
Grounding zigzag transformers	4
Auto-loops	2
Network transformers (nonlinear models)	871
Network protectors (with all the logic)	871
Unit substation transformers (nonlinear models)	20
Unit substation breakers (primary side)	20
Unit substation breakers (secondary side)	20
4 kV subnetwork breakers	107
4 kV subnetwork feeders	62
4 kV subnetwork feeder sections (mutual couplings)	3,196
Overhead transformers	109
4 kV subnetwork loads	850
High tension customer transformers (nonlinear)	37
High tension customer HV breakers	37
High tension customer LV breakers	37
High tension customer loads	11
Secondary grid sections (with mutual couplings)	17,458
Low voltage loads	6,918

TABLE IV
LOADING CONDITIONS OF THE FLUSHING NETWORK

Parameter	Units	Peak Loading	Light Loading
Active power demand	MW	386.17	237.39
Reactive power demand	Mvar	206.05	126.63
Power factor	-	0.9 (lag)	0.9 (lag)
Line charging	Mvar	41.42	41.42
Shunt capacitors	Mvar	101.05	101.05
Shunt reactors	Mvar	12.6	12.6
Total active power	MW	400.35	241.95
Total reactive power	Mvar	176.94	117.69

at 138 kV from the transmission system. Thirty primary feeders operate at 27 kV. The secondary grid includes 17 462 sections and 6918 electrical loads at 120/208 V. The Flushing network also includes a high-voltage (4 kV) subnetwork which consists of 20 unit substations interconnected by the overhead lines having 3196 three-phase sections. The distribution network also supplies power to the spot networks of large individual customers at 460 V. The configuration of this very large metropolitan network is very complex and is not shown here. Operational conditions of the Flushing network for peak and light loading conditions are given in Table IV.

IV. SIMULATION RESULTS

A. Steady-State Validation of Sutton Network Model

Before performing transient analyses of the investigated networks and drawing any conclusions, the time-domain models

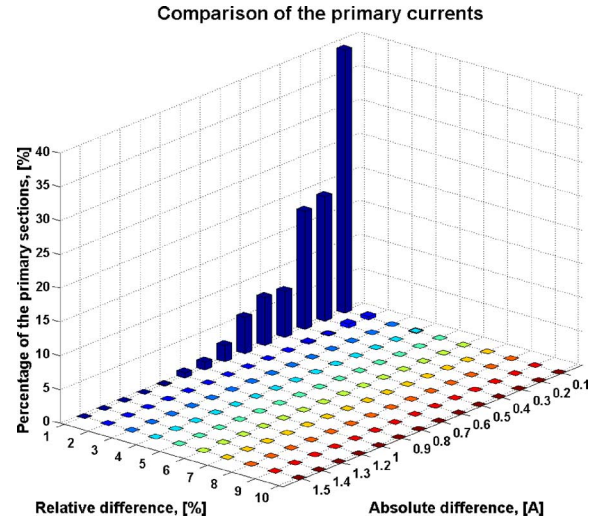


Fig. 5. Comparison of the primary currents of the Sutton network calculated using the PVL load-flow program and EMTP time-domain simulator.

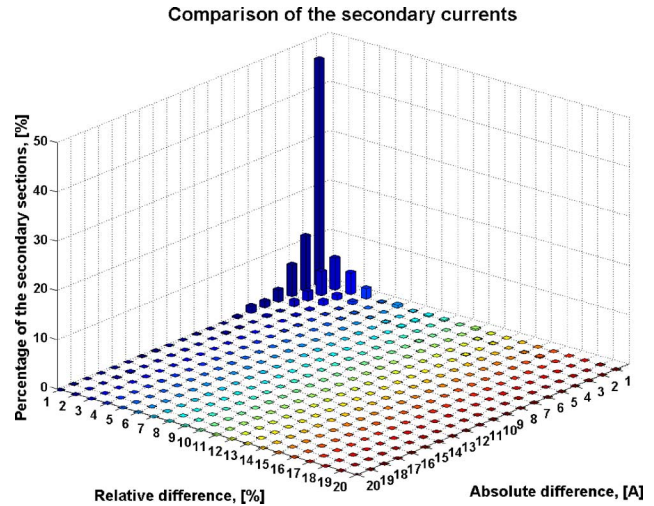


Fig. 6. Comparison of the secondary currents of the Sutton network calculated using the PVL load-flow program and EMTP time-domain simulator.

must be validated. This is due to the fact that even small modeling errors may result in significant changes in steady-state and dynamic behavior of large complex systems. Thus, to obtain accurate results, all developed custom models, introduced in Section II, were tested individually using time-domain simulations. For the sake of brevity, this process is not described here. Instead, verification of the steady-state results obtained in EMTP simulations for the complete model of the distribution network are given in more detail hereafter.

To verify the correctness of the model, a comparison tool has been written in MATLAB. It compares connectivity of the system, branch impedances, currents, and node voltages calculated using the EMTP time-domain simulations and PVL load-flow program. The comparison results for the peak loading are shown graphically in Figs. 5 and 6. As can be seen in these figures, a very good match exists between the results. Indeed, most of the relative differences in the rms values of the primary feeder currents shown in Fig. 5 are within 1%. The maximum

TABLE V
COMPARISON OF THE THREE-PHASE SHORT-CIRCUIT CURRENTS IN THE SUTTON NETWORK (FAULTS ARE IN THE PRIMARY SUBNETWORK)

Fault Location	PVL Current, [kA]	EMTP Current, [kA]	Relative Difference, [%]
Beginning of the feeder	30.5	30.7	0.65
Middle of the feeder branch 2	19.3	19.7	2.07
End of the feeder branch 3	19.8	20.3	2.52

TABLE VI
COMPARISON OF THE THREE-PHASE SHORT-CIRCUIT CURRENTS IN THE SUTTON NETWORK (FAULTS ARE IN THE SECONDARY SUBNETWORK)

Fault Location	PVL Current, [kA]	EMTP Current, [kA]	Relative Difference, [%]
Service Box	14	14.5	3.57
Vault	81.4	84.6	3.93

relative difference is 3.5%. It corresponds to the absolute current difference of only 0.07 A. At the same time, the maximum absolute difference of 0.92 A introduces only 0.6% of the relative error in the rms value of the primary feeder current. Differences in the calculated secondary grid currents are given in Fig. 6. Most of these differences are within a few percent. The largest relative difference of 18.1% corresponds to 0.64 A of the absolute current difference. The maximum absolute difference is 18 A, but it makes up slightly less than 1% of the relative difference. The small differences are attributed to two reasons: 1) numeric inaccuracy of the specific database impedances used for the netlist generation and 2) the display of few significant digits in the load-flow results of PVL.

As was mentioned previously, the Sutton network has 2333 three-phase nodes. The maximum relative difference of the voltages in all of these nodes is 0.029%. Similar comparison results were obtained for the light loading case proving the validity of the derived dynamic model.

The validation of the EMTP simulation results against the PVL output has been carried out for the cases of three-phase short circuits in the primary and secondary subnetworks. In the primary subnetwork, three fault locations were chosen at the following points:

- 1) head of the feeder (area substation bus);
- 2) middle of the feeder branch 2;
- 3) end of the feeder branch 3 (primaries of the most distant network transformer).

A comparison of the fault currents for one of the primary feeders is presented in Table V. In the secondary subnetwork, three-phase short circuits were simulated at service boxes and transformer vaults. The obtained results for two of them are given in Table VI. A maximum relative difference between node voltages obtained using EMTP and PVL was below 0.05% for all of the cases of the three-phase short circuits in primary and secondary subnetworks.

It should be noted that in the present work that the load-flow solution of the EMTP was not used. This is because the EMTP-RV does not have steady-state models (for use in the load flow) of network protectors. Instead, the time-domain (steady-state) results of the EMTP are compared at every step

of the automatic network reconfiguration. The PVL program is capable of updating the system model iteratively based on the status of every network protector in the network. As a result, using the obtained currents and voltages, it was possible to confirm that hundreds of these devices, which were accurately modeled in EMTP, operate correctly in time domain and in accordance with PVL.

As was mentioned previously, the EMTP models of the real-life distribution networks, which were described here, are used to design and implement smart grid, investigate penetration of distributed generation and develop operational strategies for these new conditions. For such studies, a large number of synchronous machine models should be properly initialized. It was shown in [24] that this goal can be promptly achieved using the EMTP load-flow solution. For validation purposes, the results will also be compared to the initial PVL solution in a sequel paper.

B. Transient Analysis Using the Sutton Network Model

In order to verify the correctness of the produced results, some real transient events that took place in the Sutton distribution network were simulated. The simulation output has been compared with actual electrical signals recorded at the secondary side of the area substation transformer by PQNode hardware [27] and processed in PQView software [28]. Some of the obtained results are presented below.

The first case consists of a single-line-to-ground fault that has occurred at the terminals of a network transformer. The transformer is supplied from the underground feeder as shown schematically in Fig. 7. This feeder is one of the 12 primary feeders connected to the 13.8-kV bus between substation transformer TR2 and synchronization bus SYN BUS SOUTH depicted in Fig. 1. A measurement unit is installed at the secondary side of the area substation transformer TR2 and records phase and neutral currents and voltages. Based on available measured data, the network loading used in the simulation has been adjusted in order to match the prefault values of currents and voltages at the transformer terminals. The simulation starts at steady-state operating conditions. A single-phase-to-ground short circuit occurs in phase A of the network transformer at 34.5 ms. This fault is isolated after approximately 6 cycles of the fundamental frequency by the corresponding feeder breaker tripping and network protector openings. The simulation and measurement results are compared in Figs. 8–15.

It may be concluded from the waveform analysis that the EMTP simulation has successfully reproduced not only the prefault, fault, and postfault behavior at the low frequencies, but it also has captured the high-frequency phenomena. For example, the first peaks of the simulated and measured fault currents marked in Fig. 9 have a difference of only 5.4% (3781.7 A versus 3997.2 A). These peaks are shown in Fig. 10 in more detail. One may notice that in this figure the maximum magnitudes of the simulated and measured currents were obtained at the same time instant (39.6 ms). As can be seen in Fig. 11, the single-phase fault in phase A results in the transient overvoltage in phase B. An enlarged picture of this transient is given in Fig. 12. A relative difference between the measured peak voltage and the simulated one is slightly less

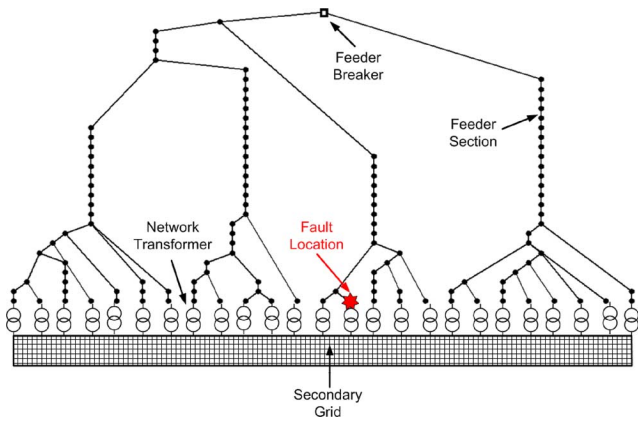


Fig. 7. Location of a single-phase-to-ground short circuit.

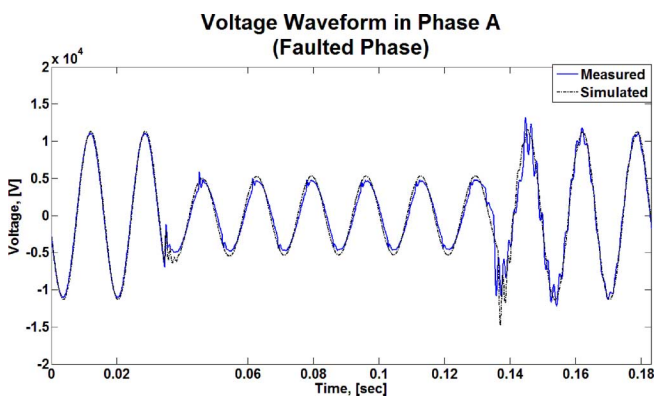


Fig. 8. Phase A (faulted phase) voltage at the secondary terminals of the area substation transformer.

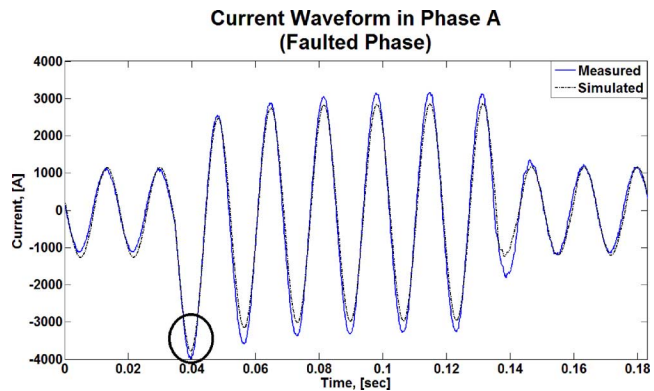


Fig. 9. Phase A (unfaulted phase) current at the secondary terminals of the area substation transformer.

than 7% (17,135 V versus 15,942 V). Once again, these values were achieved at exactly the same time instant (35.09 ms). After a complete isolation of the single-line-to-ground fault at approximately 135 ms, the oscillatory transients with very close frequencies of the oscillations can be observed in Figs. 8, 11, and 14.

In the second case presented in this paper, two consecutive single-line-to-ground faults occurred in phases A and B at the terminals of two adjacent network transformers shown in Fig. 16. As in the previous case, voltage and current records were obtained from the measurement unit installed at the secondary

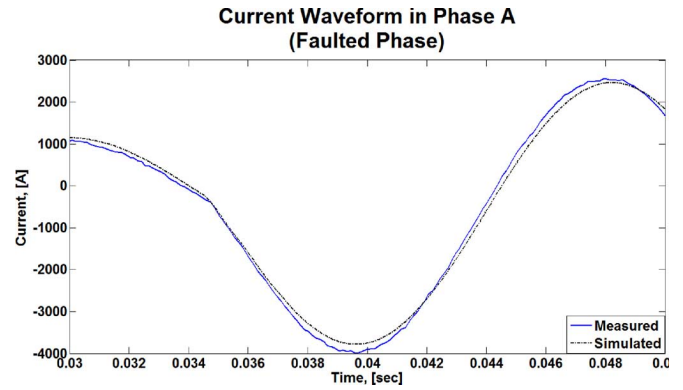


Fig. 10. First peak of the fault current in phase A at the secondary terminals of the area substation transformer.

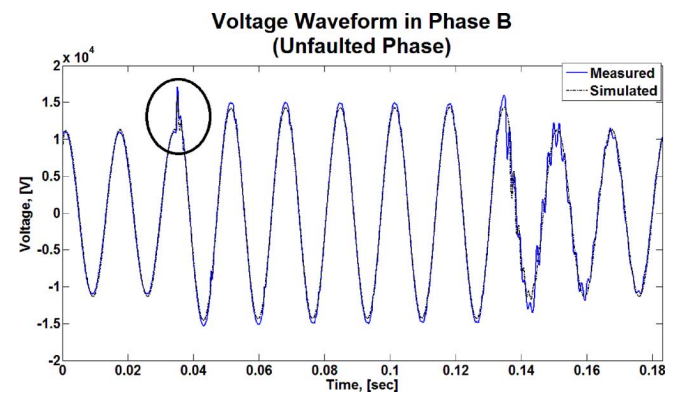


Fig. 11. Phase B (unfaulted phase) voltage at the secondary terminals of the area substation transformer.

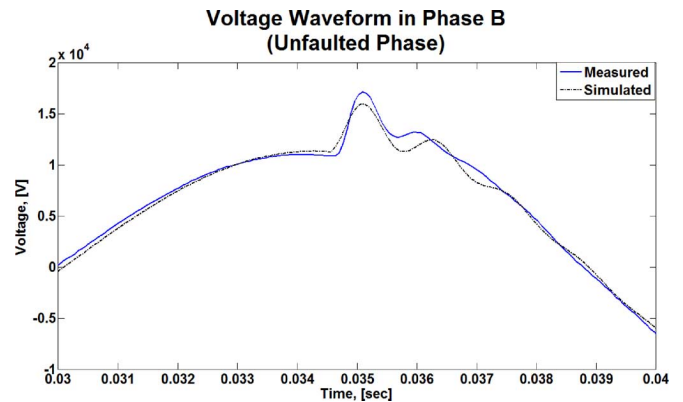


Fig. 12. Phase B (unfaulted phase) voltage at the secondary terminals of the area substation transformer (zoomed in).

side of the substation transformer TR2. Again, all voltage and current waveforms were successfully reproduced in the EMTF simulation. Indeed, as can be seen in Figs. 17–19, the simulated currents repeat the behavior of the measured ones very closely. A single-phase-to-ground short circuit occurred in phase A of the first network transformer at a time instant of 41.67 ms. This causes excessive current to flow in phase A of the area substation transformer TR2. A comparison of the corresponding measured and simulated current waveforms is presented in Fig. 17. A second single-phase-to-ground short circuit was detected by the PQNode at time instant 130.1 ms in phase B of the second

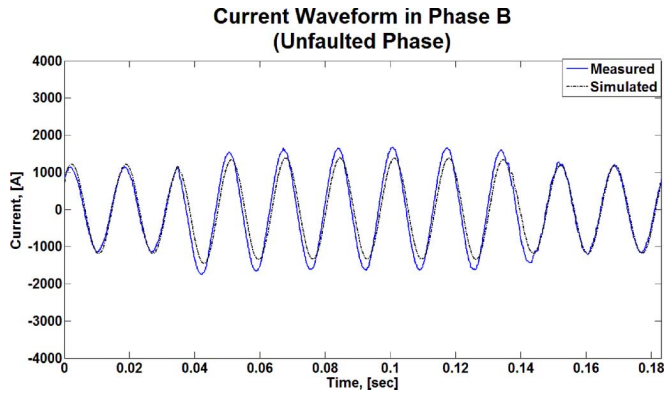


Fig. 13. Phase B (unfaulted phase) current at the secondary terminals of the area substation transformer.

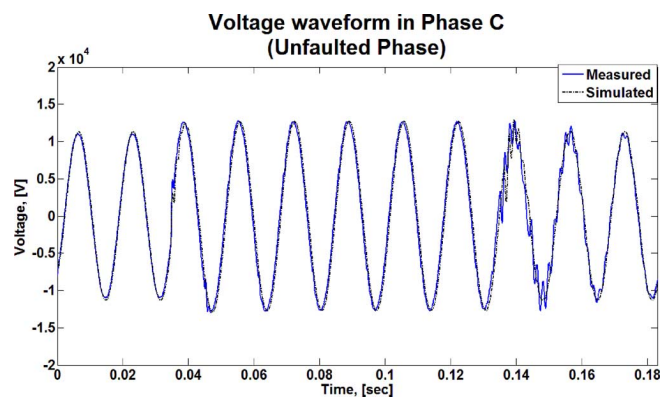


Fig. 14. Phase C (unfaulted phase) voltage at the secondary terminals of the area substation transformer.

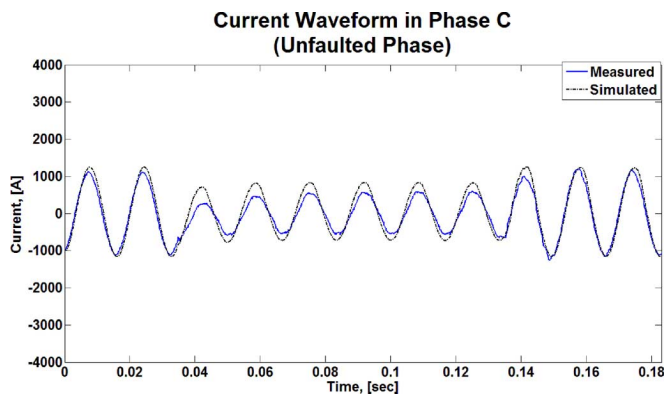


Fig. 15. Phase C (unfaulted phase) current at the secondary terminals of the area substation transformer.

network transformer depicted in Fig. 16. The current waveform of this phase recorded at the secondary side of the area transformer is also properly reproduced in the time-domain simulation of the developed EMTP model as can be seen in Fig. 18. The results shown in Fig. 19 demonstrate a good match between the measured and simulated currents in phase C.

The presented validation technique and time-domain analysis method have also been applied to the Flushing network described previously in the text and two more distribution networks of Con Edison: Randall's Island and Fordham. These

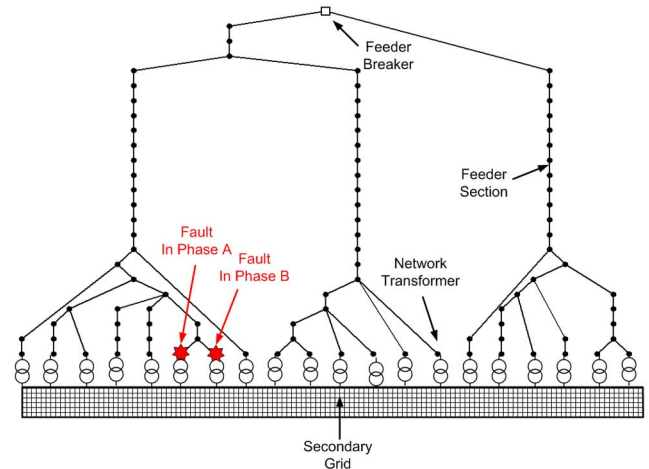


Fig. 16. Location of two single-phase-to-ground short circuits at the terminals of two adjacent network transformers.

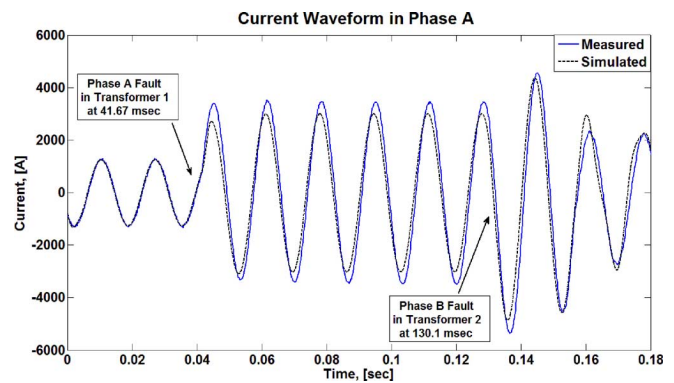


Fig. 17. Phase A (faulted phase) current at the secondary terminals of the area substation transformer in the case of two single-line-to-ground faults.

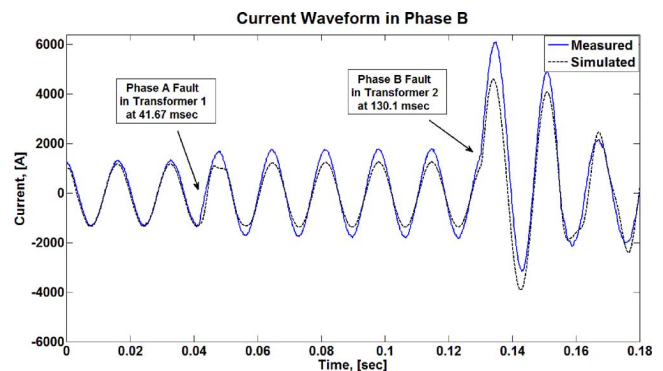


Fig. 18. Phase B (faulted phase) current at the secondary terminals of the area substation transformer in the case of two single-line-to-ground faults.

networks have different structures, configurations, and size. However, for all of these networks, the EMTP simulation results matched the load-flow output and actual measurements under different loading conditions, contingencies, as well as symmetrical and asymmetrical short circuits. Each real-life fault scenario has been accurately reproduced in the simulation including proper operation of the highly complex relay protection schemes.

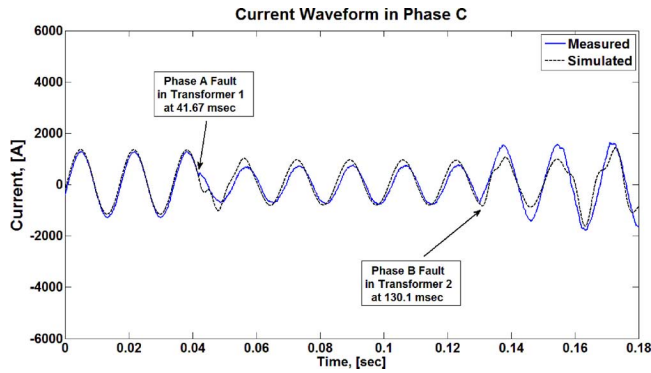


Fig. 19. Phase C (unfaulted phase) current at the secondary terminals of the area substation transformer in the case of two single-line-to-ground faults.

TABLE VII
NETWORK DATA SUMMARY

Name	Number of elements	
	Sutton	Flushing
Control-system signals	105,420	592,857
Network devices	116,379	674,027
Network nodes	10,561	87,263
Size of the main system of equations	14,851	104,825
Actual number of non-zeros	90,943	787,089
Number of data lines	342,642	2,124,726

V. MODEL COMPLEXITY AND SIMULATION TIMING

In this paper, all of the EMTP simulations were carried out using a PC computer having an Intel Core i7 CPU 975 processor operating at 3.33 GHz and installed RAM memory of 24 GB. Although the processor has eight cores, only one of them was exploited at a time since the current version of EMTP-RV does not support parallel computations. The integration step in all of the simulations was chosen to be equal to $65.1 \mu\text{s}$ (256 points per fundamental period) in order to match the sampling time of the PQNode measurement unit. The total simulation time of each EMTP simulation was equal to 183.3 ms (11 periods at the fundamental frequency) to exactly match the buffer of the measurement unit.

The network data summary for the Sutton and Flushing distribution networks is given in Table VII. It was extracted from the EMTP report and lists the number of control system signals, number of network nodes, number of devices, etc. Analyzing this data one may notice the tremendous size of the simulated models. Indeed, they include several hundreds of thousands of control-system signals and network devices, and tens of thousands of nodes. As a result, at each integration step in the time domain, very large systems of equations should be solved iteratively. In order to do it, EMTP-RV exploits the Newton algorithm which enables keeping a mean number of iterations for each integration step small [32]. In all of the simulations, this parameter was smaller than 1.38 for the Sutton network and smaller than 1.99 for the Flushing network. The largest network reported so far in the literature had a size of the system matrix of about 12 000 with a number of its nonzero elements equal to 50 269 [24]. The size of the systems of equations for the

TABLE VIII
SIMULATION STATISTICS

Solution stage	Elapsed CPU time, [s]	
	Sutton	Flushing
Data preparation	3.71	22.25
Data reading	0.09	0.47
Steady-state solution	0.53	29.79
Time-domain vector B updating	1.42	92.46
Time-domain $Ax=B$ solution	210.89	17,005.52
Control system solution	1,035.57	8,913.88
Time-domain history updating	36.78	930.83
Time-domain solution	1,441.01	34,923.30
TOTAL	1,918.81	57,288.81
	~32 min	~15 hours and 55 min

Flushing network is about 8.73 times larger whereas the number of its nonzeros is 15.66 times larger.

Finally, the elapsed CPU time required to complete each one of the simulations should be analyzed. The detailed simulation statistics as reported by EMTP-RV are given in Table VIII. Here, it can be observed that the total time required to simulate the Flushing network was 24.23 times longer than that required to obtain the solution for the Sutton network. At the same time, the main system of equations of Flushing is only 7.06 times larger than that of Sutton. The number of non-zeros is 8.65 times larger.

VI. CONCLUDING REMARKS

This paper has presented a new approach to accurately model and simulate very large electrical distribution networks in the time domain. It was shown that the proposed technique is suitable for transient and steady-state analyses of real-life systems with a detailed representation of their power and control components. The obtained simulation results have been verified against the output of the load-flow program used by the distribution company and field measurements. Good match has been found between simulations and recordings of several real transient events. The dynamic models derived in this paper can be used for the investigation of the distributed generation impact on the network operation and the development of the smart grid concepts.

ACKNOWLEDGMENT

The authors would like to thank Prof. J. Mahseredjian from École Polytechnique de Montréal for providing continuous technical support and enhanced versions of the EMTP-RV software.

REFERENCES

- [1] Y. J. Jeon, J. C. Kim, J. O. Kim, J. R. Shin, and K. Y. Lee, "An efficient simulated annealing algorithm for network reconfiguration in large-scale distribution systems," *IEEE Trans. Power Del.*, vol. 17, no. 4, pp. 1070–1078, Oct. 2002.
- [2] A. Coelho and M. G. Da Silva, "Distribution network reconfiguration with reliability constraints," in *Proc. Int. Conf. Power Syst. Technol.*, Nov. 21–24, 2004, pp. 1600–1606.
- [3] H. M. Khodr, J. Martinez-Crespo, M. A. Matos, and J. Pereira, "Distribution systems reconfiguration based on OPF using benders decomposition," *IEEE Trans. Power Del.*, vol. 24, no. 4, pp. 2166–2176, Oct. 2009.

- [4] S. Conti, "Analysis of distribution network protection issues in presence of dispersed generation," *Electr. Power Syst. Res.*, vol. 79, no. 1, pp. 49–56, Jan. 2009.
- [5] P. Trichakis, P. C. Taylor, P. F. Lyons, and R. Hair, "Predicting the technical impacts of high levels of small-scale embedded generators on low-voltage networks," *Inst. Eng. Technol. Renew. Power Gen.*, vol. 2, no. 4, pp. 249–262, 2008.
- [6] D. Singh, R. K. Misra, and D. Singh, "Effect of load models in distributed generation planning," *IEEE Trans. Power Syst.*, vol. 22, no. 4, pp. 2204–2212, Nov. 2007.
- [7] M. Thompson and D. G. Infield, "Impact of widespread photovoltaics generation on distribution systems," *Inst. Eng. Technol. Renew. Power Gen.*, vol. 1, no. 1, pp. 33–40, 2007.
- [8] C. J. Dent, L. F. Ochoa, and G. P. Harrison, "Network distributed generation capacity analysis using OPF with voltage step constraints," *IEEE Trans. Power Syst.*, vol. 25, no. 1, pp. 296–304, Feb. 2010.
- [9] L. F. Ochoa, C. J. Dent, and G. P. Harrison, "Distribution network capacity assessment: Variable DG and active networks," *IEEE Trans. Power Syst.*, vol. 25, no. 1, pp. 87–95, Feb. 2010.
- [10] P. N. Vovos, A. E. Kiprakis, A. R. Wallace, and G. P. Harrison, "Centralized and distributed voltage control: Impact on distributed generation penetration," *IEEE Trans. Power Syst.*, vol. 22, no. 1, pp. 476–483, Feb. 2007.
- [11] L. F. Ochoa, A. Padilha-Feltrin, and G. P. Harrison, "Time-series-based maximization of distributed wind power generation integration," *IEEE Trans. Energy Convers.*, vol. 23, no. 3, pp. 968–974, Sep. 2008.
- [12] G. Celli, E. Ghiani, S. Mocci, and F. Pio, "A multiobjective evolutionary algorithm for sizing and siting of distributed generation," *IEEE Trans. Power Syst.*, vol. 20, no. 2, pp. 750–757, May 2005.
- [13] D. Q. Hung, N. Mithulananthan, and R. C. Bansal, "Analytical expressions for DG allocation in primary distribution networks," *IEEE Trans. Energy Convers.*, vol. 25, no. 3, pp. 814–820, Sep. 2010.
- [14] C. Wang and M. H. Nehrir, "Analytical approaches for optimal placement of distributed generation sources in power systems," *IEEE Trans. Power Syst.*, vol. 19, no. 4, pp. 2068–2076, Nov. 2004.
- [15] J. Mahseredjian, V. Dinavahi, and J. A. Martinez, "Simulation tools for electromagnetic transients in power systems: Overview and challenges," *IEEE Trans. Power Del.*, vol. 24, no. 3, pp. 1657–1669, Jul. 2009.
- [16] N. Watson and J. Arrillaga, *Power Systems Electromagnetic Transient Simulation*. London, U.K.: IET, 2003.
- [17] I. Xyngi, A. Ishchenko, M. Popov, and L. van der Sluis, "Transient stability analysis of a distributed network with distributed generators," *IEEE Trans. Power Syst.*, vol. 24, no. 2, pp. 1102–1104, May 2009.
- [18] R. S. Thallam, S. Suryanarayanan, G. T. Heydt, and R. Ayyanar, "Impact of interconnection of distributed generation of electric distribution systems – A dynamic simulation perspective," presented at the Power Eng. Soc. Gen. Meeting, Montreal, QC, Canada, Jun. 18–22, 2006.
- [19] Z. Miao, M. A. Choudhry, and R. L. Klein, "Dynamic simulation and stability control of three-phase power distribution system with distributed generators," in *Proc. Power Eng. Soc. Winter Meeting*, Jan. 19–22, 2002, pp. 1029–1035.
- [20] S. T. Mak, "Propagation of transients in a distribution network," *IEEE Trans. Power Del.*, vol. 8, no. 1, pp. 337–343, Jan. 1993.
- [21] J. A. Martinez and J. Martin-Arnedo, "Voltage sag stochastic prediction using an Electromagnetic Transients Program," *IEEE Trans. Power Del.*, vol. 19, no. 4, pp. 1975–1982, Oct. 2004.
- [22] B. W. Lee and S. B. Rhee, "Test requirements and performance evaluation for both resistive and inductive superconducting fault current limiters for 22.9 kV Electric Distribution Network in Korea," *IEEE Trans. Appl. Superconduct.*, vol. 20, no. 3, pp. 1114–1117, Jun. 2010.
- [23] DCG-EMTP (Development coordination group of EMTP) Version EMTP-RV, Electromagnetic Transients Program. [Online]. Available: <http://www.emtp.com>
- [24] L. Gérin-Lajoie and J. Mahseredjian, "Simulation of an extra large network in EMTP: From electromagnetic to electromechanical transients," presented at the Int. Conf. Power Syst. Transients, Kyoto, Japan, Jun. 2–6, 2009.
- [25] J. Mahseredjian, S. Denetière, L. Dubé, B. Khodabakhchian, and L. Gérin-Lajoie, "On a new approach for the simulation of transients in power systems," in *Proc. 6th Int. Conf. Power Syst. Transients, Elect. Power Syst. Res.*, Sep. 2007, vol. 11, pp. 1514–1520, 77.
- [26] Technical Computing Software. MATLAB. The MathWorks, Inc. [Online]. Available: <http://www.mathworks.com>
- [27] *IEEE Standard Requirements for Secondary Network Protectors*, IEEE Standard C57.12.44, 2005.
- [28] *IEEE Standard for AC High-Voltage Circuit Breakers Rated on a Symmetrical Current Basis – Preferred Ratings and Related Required Capabilities for Voltages Above 1000 V*, IEEE Standard C37.06, 2009.
- [29] B. Kovan, F. de León, D. Czarkowski, Z. Zabar, and L. Birenbaum, "Mitigation of inrush currents in network transformers by reducing the residual flux with an ultra-low-frequency power source," *IEEE Trans. Power Del.*, vol. 26, no. 3, pp. 1563–1570, Jul. 2011.
- [30] Dranetz, Power quality instrumentation, PQNode. [Online]. Available: <http://dranetz.com/>
- [31] Elektrotek Concepts, Power quality database management and analysis software. PQView. [Online]. Available: <http://www.elektrotek.com/pqview.htm>
- [32] J. Mahseredjian, L. Dubé, M. Zou, S. Denetière, and G. Joos, "Simultaneous solution of control system equations in EMTP," *IEEE Trans. Power Syst.*, vol. 21, no. 1, pp. 117–124, Feb. 2006.

Vitaly Spitsa (M'10) received the M.Sc. and Ph.D. degrees in electrical engineering from Technion - Israel Institute of Technology, Haifa, Israel, in 2002 and 2009, respectively.

He has been a Control and Algorithm Engineer with a motion control company in Israel. Currently, he is a Research Assistant Professor at Polytechnic Institute of New York University, Brooklyn, NY. His research interests are in the areas of power system analysis, electrical machines, drives and robust control.

Reynaldo Salcedo (S'09) received the B.Sc. and M.Sc. degrees in electrical engineering from Polytechnic Institute of New York University, Brooklyn, NY, in 2010 and 2011, respectively, where he is currently pursuing the Ph.D. degree in electrical engineering.

His current research area is power system modeling and analysis.

Xuanchang Ran received the B.Sc. degree in electrical engineering from Southwest Jiaotong University, Chengdu, China, in 2008, and the M.Sc. degree in electrical engineering from Polytechnic Institute of New York University, Brooklyn, NY, in 2010, where he is currently pursuing the Ph.D. degree.

His research interest is power system analysis and power theory.

Juan F. Martínez (M'11) received the B.Sc. degree in electrical engineering from Grove School of Engineering - The City College of New York, New York, in 2008.

Currently, he is an Engineering Supervisor with Consolidated Edison Company of New York. His research interest is in the area of power system analysis.

Resk Ebrahim Uosef (M'01) received the B.Sc. and M. Sc. degrees in electrical engineering from Alexandria University Faculty of Engineering, Alexandria, Egypt, in 1979 and 1981, respectively. He received a second M.Sc. degree in electrical engineering from Polytechnic University, Brooklyn, NY, in 2007, along with the Ph.D. degree in 2011.

He was an Engineer in a hydropower generating station in Egypt, and then he was the Owner of a consulting firm for an electric construction company in Egypt. He joined Con Edison's Distribution Engineering Department in 2003 and is currently responsible for Con Edison's distribution system design and analysis.

Dr. Uosef is a registered professional engineer in the State of New York.

Francisco de León (S'86–M'92–SM'02) received the B.Sc. and the M.Sc. (Hons.) degrees in electrical engineering from the National Polytechnic Institute, Mexico City, Mexico, in 1983 and 1986, respectively, and the Ph.D. degree from the University of Toronto, Toronto, ON, Canada, in 1992.

He has held several academic positions in Mexico and has worked for the Canadian electric industry. Currently, he is an Associate Professor at the Polytechnic Institute of New York University, New York. His research interests include the analysis of power phenomena under nonsinusoidal conditions, the transient and steady-state analyses of power systems, the thermal rating of cables, and the calculation of electromagnetic fields applied to machine design and modeling.

Dariusz Czarkowski (M'97) received the M.Sc. degree in electronics from the University of Mining and Metallurgy, Krakow, Poland, in 1989, the M.Sc. degree in electrical engineering from Wright State University, Dayton, OH, in 1993, and the Ph.D. degree in electrical engineering from the University of Florida, Gainesville, in 1996.

In 1996, he joined the Polytechnic Institute of New York University, Brooklyn, NY, where he is currently an Associate Professor of Electrical and Computer Engineering. He is a coauthor of *Resonant Power Converters* (Wiley, 1995). His research interests are in the areas of power electronics, electric drives, and power quality.

Dr. Czarkowski has served as an Associate Editor for the IEEE TRANSACTIONS ON CIRCUITS AND SYSTEMS.

Zivan Zabar (M'76–SM'81) was born in Hadera, Israel, in 1939. He received the B.Sc., M.Sc., and D.Sc. degrees from Technion–Israel Institute of Technology, Haifa, Israel, in 1965, 1968, and 1972, respectively.

He is currently a Professor of Electrical Engineering at the Polytechnic Institute of New York University, Brooklyn, NY. He served as the Head of the Electrical and Computer Engineering Department at the Polytechnic Institute of New York University for three years (1995–1998). He has six patents and more than 50 papers published in technical journals. His areas of interest are electric power systems, electric drives, and power electronics.

Dr. Zabar is a member of Sigma Xi.